OPTIMAL ANALOG WAVELET BASES CONSTRUCTION USING HYBRID OPTIMIZATION ALGORITHM

Hongmin Li [1, 2], Yigang He[2], Yichuang Sun[3]

[1.] College of Physical and Electronic Engineering, Hunan Institute of Science and Technology, Yueyang 414006, China, lihminnew@sina.com

[2.] College of Electrical and Automation Engineering, Hefei University of Technology, Hefei 230009, China

[3.] School of Electronic, Communication and Electrical Eng., University of Hertfordshire, Hatfield ALl0 9AB, UK

Submitted: April 29, 2016 ***Accepted: Oct.17, 2016*** ***Published: Dec.1, 2016***

Abstract- An approach for the construction of optimal analog wavelet bases is presented. First, the definition of an analog wavelet is given. Based on the definition and the least-squares error criterion, a general framework for designing optimal analog wavelet bases is established, which is one of difficult nonlinear constrained optimization problems. Then, to solve this problem, a hybrid algorithm by combining chaotic map particle swarm optimization (CPSO) with local sequential quadratic programming (SQP) is proposed. CPSO is an improved PSO in which the saw tooth chaotic map is used to raise its global search ability. CPSO is a global optimizer to search the estimates of the global solution, while the SQP is employed for the local search and refining the estimates. Benefiting from good global search ability of CPSO and powerful local search ability of SQP, a high-precision global optimum in this problem can be gained. Finally, a series of optimal analog wavelet bases are constructed using the hybrid algorithm. The proposed method is tested for various wavelet bases and the improved performance is compared with previous works.

Index Terms- Wavelet transform, Analog wavelet base, Optimization methods, Particle swarm optimization (PSO), Saw tooth chaotic map, Sequential quadratic programming (SQP).

I. INTRODUCTION

The Wavelet Transform (WT) has been proven very useful in many fields due to the ability of wavelets to resolve localized signal content in both scale and space [1-5]. The conventional method of implementing WT is by means of digital signal processing systems (DSP) with the required A/D or D/A converters. For WT, emerging applications such as low power sensor networks [6]and [7], next-generation cochlear implants [8] and [9], and implantable pacemakers [10]continue to challenge its implement method with ever more stringent requirements-ultra low power cost, very small size, and real-time performance. With modern advances in the area of programmable and reconfigurable analog VLSI technologies, it is feasible to implement complex signal processing employing analog systems with very low power and small size [13-18]. Application requirements and novel analog circuit technologies provide a motivation for realizing WT based on analog systems, and a number of attempts have been made so far.

Previous studies on analog hardware implementation of WT can be divided into two categories, namely time-domain approach [19-21] and frequency-domain approach [22-31]. The latter is now the mainstream approach and the performance of such implementation primarily depends on the accuracy of the corresponding wavelet approximations. In fact, it is a nonlinear constrained optimization problem to approximate wavelets. Some approaches based on optimization techniques for wavelet approximations have been reported, which include mainly L2 approximation method [26], network function method [23],[25], differential evolution method [30], [31] and simulated annealing method [31]. However, these methods are difficult to ensure a global initial value, which may result in a local optimal result. So, some more effective technologies to get optimal wavelets for analog hardware implementation should be explored.

In this paper, we are interested in the analog hardware implementation frequency -domain of WT and the constructing the optimal analog wavelets. The innovative aspects of this paper are threefold. First, by extending author's previous work [27] and [28] we propose a general framework of constructing optimal analog wavelet bases. Based on linear system theory and wavelet transform theory, the definition of analog wavelet base is given. Then applying the least-squares error criterion, mathematical model of designing optimal analog wavelet bases is established, which is a typical complex function nonlinear constrained optimization problem. Second, a hybrid optimization algorithm by combining chaotic map Particle Swarm Optimization

[33] (CPSO) with local sequential quadratic programming (SQP) [32] is presented to solve the optimization problem. CPSO is an improved PSO in which the saw tooth chaotic map is used to avoid premature problem of PSO and raise its global search ability. Finally, based on the proposed hybrid algorithm and the general frame, a series of optimal analog wavelet bases are constructed. CPSO is a stochastic optimization technique with powerful global search ability. Using CPSO to find a global initial value for SQP which is a powerful nonlinear programming algorithm, we can get high-precision optimal analog wavelets and overcome these limitations in previous methods. Experimental results confirmed this.

The paper is organized as follows: In sections 2, we give the definition of analog wavelet base. In sections 3, the general frame of constructing optimal analog wavelet bases is set up. In sections 4, we propose a hybrid optimization algorithm by combining CPSO and SQP. In sections 5, we construct many optimal analog wavelet bases using the proposed hybrid algorithm, and compare the performance of proposed method with other method.

II. ANALOG WAVELET TRANSFORM AND ANALOG WAVELET BASE

The definition of the continuous wavelet transform (CWT) for a real valued time signal $x(t)$ is given as [2]

$$\mathrm{WT}_x(a,\tau)=\frac{1}{\sqrt{a}}\int_{-\infty}^{\infty}x(t)\psi^*(\frac{t-\tau}{a})dt \qquad (1)$$

where a is scale parameter ($a\in(0,\boldsymbol{R})$) and τ is translation parameter ($\tau\in\boldsymbol{R}$). The basis function $\psi(t)$ ($\psi(t)\in L(\boldsymbol{R})^2$) is called the mother wavelet or wavelet base. The mother wavelet used to generate all the basis functions is designed based on some desired characteristics associated with that function. The translation parameter τ relates to the location of the wavelet function as it is shifted through the signal. The wavelet base must satisfy two restriction conditions. One is

$$\int_{-\infty}^{\infty}\psi(t)dt=0 \qquad (2)$$

This ensures the mother wavelet has no DC component and is fast in decaying rate. The other is the admissibility condition, i.e.

$$\int_{-\infty}^{\infty} \frac{|\Psi(w)|^2}{|w|} dw < \infty \qquad (3)$$

where $\Psi(w)$ is the Fourier transform of the mother wavelet $\psi(t)$. The second restriction in equation (3) is stronger than the first one. The reason for requiring this condition is to guarantee that the reconstruction of the original time signal from the continuous wavelet transform is possible.

The above equation (1) shows that the wavelet transform performs the convolution operation of the signal and the basis function. Let $1/\sqrt{a}\psi(-t/a)$ be a linear analog filter impulse response $h(t)=1/\sqrt{a}\psi(-t/a)$, then $\mathrm{WT}_x(a,\tau)$ of signals under scale a can be achieved through the implementation of a linear analog filter. Here, the linear filter $h(t)$ is called analog wavelet filter. So, by transforming equation (1), we can obtain the definition of analog wavelet transform:

$$\mathrm{WT}_{xA}(a,\tau) = x(t) * \frac{1}{\sqrt{a}} \psi_A(-\frac{t}{a}) \qquad (4)$$

where $\psi_A(t)$ is the analog wavelet base and $*$ denotes the convolution. Figure 1 shows analog wavelet transform realization block diagram using analog filter banks.

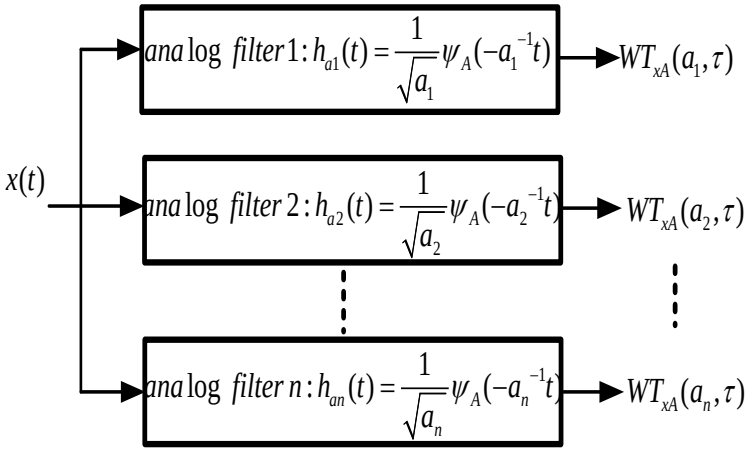

Figure 1. Block diagram of analog wavelet transform

For obvious physical reasons, only the analog hardware implementation of causal stable filters is feasible. Thus, analog wavelet bases must satisfy some other conditions besides the admissibility condition. First, $\psi_A(-t)$ needs to possess a rational Laplace transform, i.e.

$$H(s)=\int_R \psi_A(-t)e^{-st}dt=\frac{b_m s^m+\cdots+b_1 s+b_0}{s^n+a_{n-1}s^{n-1}\cdots+a_1 s+a_0} \tag{5}$$

which has all its poles in the complex left half plane. Second, $\psi_A(-t)$ is causal signal. In other word, $\psi_A(t)$ must be zero for positive t. From the discussion described above, we define the analog wavelet base as follows:

Definition 1 The function $\psi_A(t)$ is an analog wavelet base if $\psi_A(t)$ satisfies all following conditions:

$$\begin{cases} 1)\ \psi_A(t)\in L^2(R) \\ 2)\ C_\Psi=\int_R \frac{\left|\Psi_A(w)\right|^2}{|w|}\,dw<\infty \ or \int_{-\infty}^{\infty}\psi_A(t)dt=0 \\ 3)\ \int_0^{\infty}\psi_A(-t)e^{-st}dt=\frac{b_m s^m+\cdots+b_1 s+b_0}{s^n+a_{n-1}s^{n-1}\cdots+a_1 s+a_0} \\ 4)\ \int_{-\infty}^{\infty}|\psi_A(-t)|^2\,dt<\infty\ ,\quad 5)\ \psi_A(t)=0,\ t>0 \end{cases} \tag{6}$$

Up to now, various versatile wavelet bases with excellent qualities have been designed since the wavelet transform theory was put forward, such as Marr wavelet, Gaussian wavelet, and Morlet wavelet, etc. and have been successfully applied to the signal processing and analysis [1]. However, these versatile wavelets usually do not satisfy some conditions for analog wavelets in equation (6). In order to meet new application requirements for low-power, small size and real-time, how to construct analog wavelet bases as fine as versatile wavelets has gradually become a popular research topic.

III. THE GENERAL FRAMEWORK OF CONSTRUCTING OPTIMAL ANALOG WAVELET BASES

To obtain analog wavelet bases with excellent properties, we naturally think of the approach method. If the analog wavelets constructed can approach the versatile wavelet well in time domain, we will easily find good analog wavelet bases. According to the linear system theory, a analog wavelet base $\psi_A(t)$ possessing the Laplace transform expression in Eq.(5) may typically

have the following form:

$$\psi_A(t) = \sum_{i=1}^{k} a_i e^{b_i t} + \sum_{j=1}^{m} [c_j e^{d_j t} \sin(-f_j t) + g_j e^{d_j t} \cos(-f_j t)] \quad (k+2m = N, t \le 0) \tag{7}$$

where the parameters b_i and d_j must be strictly negative for reasons of stability, and N is the order of analog wavelet filter. When the expression of desired versatile wavelet includes cosine term $A\cos(\Omega t)$ (or $A\sin(\Omega t)$), such as the Morlet wavelet, the $\Psi_A(t)$ may be given by:

$$\psi_A(t) = [\sum_{i=1}^{k} a_i e^{-b_i t} + \sum_{j=1}^{m} [c_j e^{-d_j t} \sin(f_j t) + g_j e^{-d_j t} \cos(f_j t)]] \cos(\Omega(t_0 + t)) \quad (2k+2m = N, t \le 0) \tag{8}$$

Note above expression only can get wavelet filter with even order. If to design the odd order one, we only need to move the term $\sum a_i e^{-b_i t}$ to the outside of the bracket and transform the form of equation (8). Let $\varepsilon^2(\boldsymbol{a,b,c,d,f,g})$ be the least-squares error between $\psi_A(-t)$ and $\psi(-t+t_0)$ (time-shifted versatile wavelet), then

$$\varepsilon^2(\boldsymbol{a,b,c,d,f,g}) = \left\| \psi_A(-t) - \psi(-t+t_0) \right\|^2 = \int_{-\infty}^{\infty} \left| \psi_A(-t) - \psi(-t+t_0) \right|^2 dt \tag{9}$$

where $\boldsymbol{a} = (a_1 \quad a_2 \quad a_3 \cdots a_k)^T$, $\boldsymbol{b} = (b_1 \quad b_2 \quad b_3 \cdots b_k)^T$、$\boldsymbol{c} = (c_1 \quad c_2 \quad c_3 \cdots c_m)^T$, $\boldsymbol{d} = (d_1 \quad d_2 \quad d_3 \cdots d_m)^T$, $\boldsymbol{f} = (f_1 \quad f_2 \quad f_3 \cdots f_m)^T$ and $\boldsymbol{g} = (g_1 \quad g_2 \quad g_3 \cdots g_m)^T$ are all undetermined parameters vectors in $\psi_A(t)$. By minimizing the $\varepsilon^2(\boldsymbol{a,b,c,d,f,g})$ in equation (9), the target to construct optimal $\psi_A(t)$ will be reached. To apply numerical optimization technologies, we sample $\varepsilon^2(\boldsymbol{a,b,c,d,f,g})$ in time with M points and obtain the sum of squares error (MSE) between the analog wavelet base and the desired versatile wavelet:

$$E(\boldsymbol{a,b,c,d,f,g}) = \sum_{n=0}^{M-1} [\psi_A(-n\Delta T) - \psi(-(n\Delta T - t_0))]^2 \tag{10}$$

The fitness function to be minimized using the numerical optimization algorithms is given:

$$F(\boldsymbol{a,b,c,d,f,g}) = E(\boldsymbol{a,b,c,d,f,g}) = \sum_{n=0}^{M-1} [\psi_A(-n\Delta T) - \psi(-(n\Delta T - t_0))]^2 \tag{11}$$

Then, combining all the conditions in equations (6)-(8), and (11), a general optimization mathematical model of constructing analog wavelet bases in time domain is described as:

$$
\begin{cases}
\min \quad F(\boldsymbol{a},\boldsymbol{b},\boldsymbol{c},\boldsymbol{d},\boldsymbol{f},\boldsymbol{g}) = \sum_{n=0}^{M-1} [\psi_A(-n\Delta T) - \psi(-(n\Delta T - t_0))]^2 \\
s.t. \quad b_i < 0, d_j < 0, i = 1,2\cdots k,\ j == 1,2\cdots m, \\
\quad \int_{-\infty}^{\infty} \psi_A(t)dt = 0, \\
\quad \psi_A(-t) = \sum_{i=1}^{k} a_i e^{-b_i t} + \sum_{j=1}^{m} [c_j e^{-d_j t} \sin(f_j t) + g_j e^{-d_j t} \cos(f_j t)] \quad or \\
\quad \psi_A(-t) = [\sum_{i=1}^{k} a_i e^{-b_i t} + \sum_{j=1}^{m} [c_j e^{-d_j t} \sin(f_j t) + g_j e^{-d_j t} \cos(f_j t)]] \cos(\Omega(t_0 - t))\ \ (k + 2m = N, t \geq 0), \\
\quad \boldsymbol{a} = (a_1 \quad a_2 \quad a_3 \cdots a_k)^T,\ \boldsymbol{b} = (b_1 \quad b_2 \quad b_3 \cdots b_k)^T, \boldsymbol{c} = (c_1 \quad c_2 \quad c_3 \cdots c_m)^T \\
\quad \boldsymbol{d} = (d_1 \quad d_2 \quad d_3 \cdots d_m)^T,\ \boldsymbol{f} = (f_1 \quad f_2 \quad f_3 \cdots f_m)^T, \boldsymbol{g} = (g_1 \quad g_2 \quad g_3 \cdots g_m)^T.
\end{cases}
\tag{12}
$$

This is a typical high-dimensional, nonlinear, multimodal complex functions nonlinear constrained optimization problem. It is very difficult to search the accurate global optimal solution using common numerical optimization techniques, which in general provide no global optimality guarantee and give different local optima with different starting points. After establishing a good mathematical model, whether we are able to get the optimal analog wavelet bases depends greatly on the performance of the optimization algorithm used to solve the problem.

IV. THE HYBRID OPTIMIZATION ALGORITHM

The methods for solving nonlinear optimization problems are mainly divided into two categories: deterministic and stochastic search algorithms. Deterministic search methods include feasible direction method, gradient projection method and local sequential quadratic programming (SQP) so on [32]. The SQP belongs to the most powerful nonlinear programming algorithms we know today for solving differentiable nonlinear programming problems with nonlinear constrains, but whether the solution is optimal or not depends greatly on the initial value. Stochastic search algorithms include simulated annealing [34], genetic algorithm (GA)[35] and recently proposed Particle Swarm Optimization (PSO) [33]etc. Although GA is a good global searching method, it is too complex in coding and time consumption. PSO characterized by its less parameter, simplicity and efficiency, being insensitive to initial value, has already been successfully used in many real-world problems [36]. The PSO is very well for global optimization, but it is not good at searching the high-precision solution. As in [37] demonstrated by Van den Bergh, PSO also

has the weakness of premature convergence like other search algorithms. The chaotic map can be used to improve the performance of standard PSO to avoid premature convergence, The proposed improved PSO based on chaotic map is called CPSO. To solve the constrained nonlinear optimization problem in equation (12), a hybrid optimization algorithm by combining CPSO with local SQP is presented. CPSO can be viewed as the global optimizer while the local SQP is employed for the local search. Thus, the possibility of exploring global optima in equation (12) with more local optima is increased. Benefit from the fast globally converging characteristics of CPSO and the effective local search ability of local SQP. Thus, the hybrid algorithm can obtain the global optimal results of optimization problem in equation (12) quickly.

a. Standard PSO Algorithm

PSO was originally inspired in the way crowds of individuals move towards predefined objectives, and it is better viewed using a social metaphor. Each potential solution is also assigned a randomized velocity, and the potential solutions, call particles, corresponding to individuals. Each particle in PSO flies in the D-dimensional problem space with a velocity which is dynamically adjusted according to the flying experiences of its own and its colleagues. The location of the *ith* particle is represented as $\boldsymbol{X}_i = (x_{i1}, \ldots, x_{id}, \ldots, x_{iD})$, where $x_{id} \in [l_d, u_d], d \in [1, D], l_d, u_d$ are the lower and upper bounds for the d th dimension, respectively. The best previous position of the *ith* particle is recorded and represented as $\boldsymbol{P}_i = (p_{i1}, \ldots, p_{id}, \ldots, p_{iD})$, which is also called pbest. The index of the best particle among all the particles in the population is represented by the symbol $\boldsymbol{Pg}$ .The location $\boldsymbol{Pg}_i = (pg_{i1}, \ldots, pg_{id}, \ldots, pg_{iD})$ is also called gbest. The velocity for the i th particle is represented as $\boldsymbol{V}_i = (v_{i1}, \ldots, v_{id}, \ldots, v_{iD})$, is clamped to a maximum velocity $\boldsymbol{V}_{max} = (v_{max1}, \ldots, v_{maxd}, \ldots, v_{maxD})$, which is specified by the user. The particle swarm optimization concept consists of, at each time step, changing the velocity and location of each particle toward its pbest and gbest locations according to the equations (13) and (14), respectively:

$$v_{id} = w \cdot v_{id} + c_1 \cdot rand() \cdot (p_{id} - x_{id}) + c_2 \cdot rand() \cdot (pg_{id} - x_{id}) \qquad (13)$$

$$x_{id} = x_{id} + v_{id} \qquad (14)$$

where w is inertia weight, c_1 and c_2 are acceleration constants, and *rand*() is a random function in the range[0, 1].

b. The improved chaotic map PSO algorithm (CPSO)

In order to overcome the premature convergence, a logistic map-based chaotic particle swarm optimization (LPSO) [38] has been described and it can lead to the effective enhancement of the searching efficiency, as well as great improvement of the searching quality. Here, we will put forward our exploration on saw tooth chaotic map [39] particle swarm optimization (CPSO), exhibiting even higher convergence and accuracy. A chaotic map is a map that exhibits some sort of chaotic behavior. Maps may be parameterized by a discrete-time or a continuous-time parameter. Discrete maps usually take the form of iterated functions. In this paper, a saw tooth chaotic map, which has better ergodic property than the well-known logistic equation, is employed for improving the global search ability of PSO. The saw tooth map is defined by the discrete-time relationship that maps present state $x(n)$ into next state $x(n+1)$ according to

$$x(n+1) = F[x(n)] = [2x(n)] \bmod 1 \qquad (15)$$

where function $F(x)$ evaluates the non-integer part of the product of present state $x(n)$ by 2. It is apparent that function $F(x)$ maps state space [0, 1] into itself.

The CPSO algorithm is outlined in the following steps:

1) Initialization: the particle swarm size is set to be I, the iteration time is set to be N, n=1, i=1, m=1, initialize velocity $\boldsymbol{V}_i$; Chaotic searching iteration number is set to be G, the premature convergence parameter is set to be η.
2) Generate I particles randomly, and compute the fitness function:
$$\boldsymbol{F}(\boldsymbol{X}_1^{(n)}), F(\boldsymbol{X}_2^{(n)}) \cdots F(\boldsymbol{X}_I^{(n)}).$$
3) Let $\boldsymbol{P}_i = \boldsymbol{X}_i^{(n)}$, $\boldsymbol{Pg} = \left\{ \boldsymbol{P}_i \mid F(\boldsymbol{P}_i) = MIN\left\{ F(\boldsymbol{X}_1^{(n)}), F(\boldsymbol{X}_2^{(n)}), \cdots, F(\boldsymbol{X}_I^{(n)}) \right\} \right\}$.
4) Let n=n+1, and compute $\boldsymbol{V}_i^{(n)}$ and $\boldsymbol{X}_i^{(n)}$ according to the formulas (13) and (14).
5) Compute $F(\boldsymbol{X}_i^{(n)})$. If $F(\boldsymbol{X}_i^{(n)}) > F(\boldsymbol{P}_i)$, go to Step6, otherwise, let $\boldsymbol{P}_i = \boldsymbol{X}_i^{(n)}$ and go to step 5).
6) If $F(\boldsymbol{X}_i^{(n)}) < F(\boldsymbol{Pg})$, let $\boldsymbol{Pg} = \boldsymbol{X}_i^{(n)}$.
7) According to equation (16), compute fitness variance σ^2 of current particles:

$$\sigma^2 = \sum_{i=1}^{I} \frac{F(\boldsymbol{X}_i^{(n)}) - F_{avg}}{FA}, \; FA = \begin{cases} \max\limits_{1 \le i \le I} \left| F(\boldsymbol{X}_i^{(n)}) - F_{avg} \right| & if \max\limits_{1 \le i \le m} \left| F(\boldsymbol{X}_i^{(n)}) - F_{avg} \right| > 1 \\ 1 & else \end{cases} \qquad (16)$$

where F_{avg} is the average fitness. If $\sigma^2 < \eta$, implement the chaotic search according to

equation (17) and (18) until n equals G, then let $\boldsymbol{Pg} = C\boldsymbol{Pg}^{(G)}$. Otherwise go to step 7).

$$\boldsymbol{Pg}^{(k+1)} = [2\boldsymbol{Pg}^{(k)}] \bmod 1 \qquad (17)$$

$$C\boldsymbol{Pg}^{(k+1)} = C\boldsymbol{Pg}_{\min} + \boldsymbol{Pg}^{(k+1)}(C\boldsymbol{Pg}_{\max} - C\boldsymbol{Pg}_{\min}) \qquad (18)$$

8) Let i=i+1. If i > I , go to step 7), otherwise go to step 3).

9) If n > N, output the result and the algorithm ends, otherwise, go to step 3).

c. Hybrid algorithm based on CPSO and local SQP

By introducing the saw tooth chaotic map, we avoid premature problem of PSO and improve its global search ability. But its local search capabilities are limited. The local SQP algorithm has strong local search ability, but it is sensitive to initial value and easy to fall into local optimum and can not obtain the global optimum. Combining the advantages of both algorithms, we proposed a novel hybrid algorithm which consists of two steps: First, employ CPSO to obtain estimates of the global solution. Secondly, applying the estimates from CPSO as the initial value, employ the local SQP algorithm to further refine the solution, and ultimately get precise global optimal solution. The flow chart of the proposed hybrid optimization algorithm is shown in Figure 2.

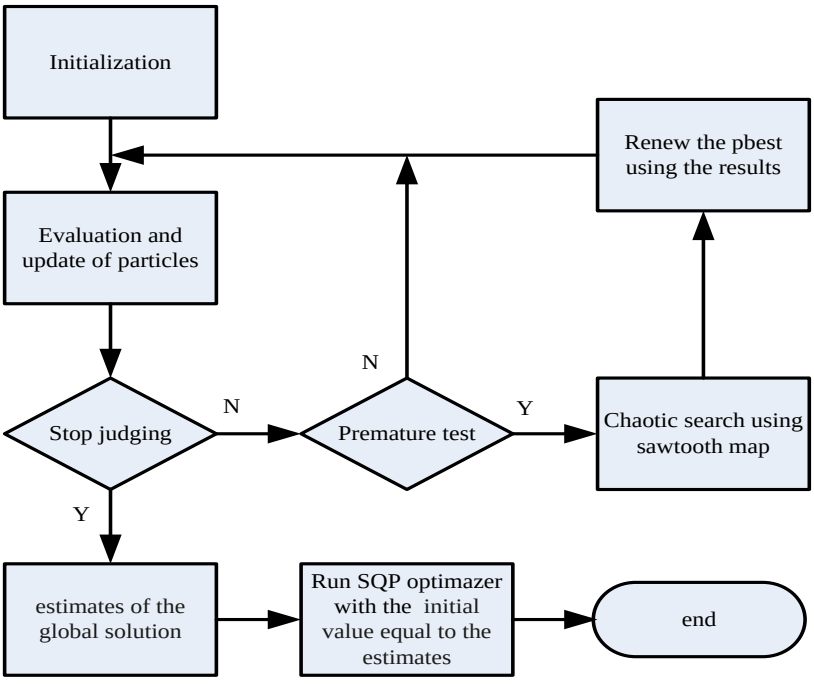

Figure 2. Flow chart of proposed hybrid optimization algorithm

d. Hybrid algorithm testing

The performance of the proposed hybrid algorithm is tested using three famous benchmark functions: schaffer function, rosenbrock function and rastrigrin function.PSO, LPSO (PSO based logistic chaotic map), and the proposed hybrid algorithm are utilized to find the minimum of above three functions respectively. For every algorithm, 30 experiments are carried out. Chaotic search numbers is set to 50 to treat premature problem in PSO. Test results are given in Table 1. It is clear that the proposed hybrid algorithm based on CPSO and local SQP is superior to the standard PSO, and the LPSO. It demonstrated that the obtained results of hybrid algorithm for the all functions are much better than the other algorithms and it can reach a high-precision global optimal solution faster. Moreover, the proposed hybrid algorithm is showing a higher capability of escaping local minima.

Table 1: Performance comparison of PSO, CPSO and hybrid algorithm

function	algorithm	optimal result	average optimal result	succeed ratio
schaffer	PSO	-0.5	-0.4121	86%
	LPSO	-0.5	-0.4578	92%
	hybrid algorithm	-0.5	-0.498	97%
rosenbrock	PSO	0.81	0.926	79%
	LPSO	0.62	0.714	88%
	hybrid algorithm	0	0.00482	96%
rastrigrin	PSO	0.089	0.1254	82%
	LPSO	0.045	0.0862	91%
	hybrid algorithm	0	0.00271	96%

V. CONSTRUCTION OF OPTIMAL ANALOG WAVELET BASES

Using the proposed hybrid algorithm to solve the problem in equation (12) and find out the global optimum, the construction of optimal analog wavelet bases will be realized. The total performing process is shown by the flowchart in Figure 3. First, determine what analog wavelet base to be

designed, for example, if you plan to construct the analog wavelet $\psi_A(t)$ with the same characteristics as the Gaussian wavelet $\psi(t)$ (versatile wavelet), Gaussian wavelet will be chosen as the approached object. Correspondingly, this analog wavelet is called Gaussian-like analog wavelet. Second, set up the optimization mathematical model for constructing analog wavelet according to equation (12). Finally, employ the proposed hybrid algorithm to solve the optimization problem and finish the construction of optimal analog wavelet bases. Based on the method, some real and complex analog wavelet bases designing will be discussed as follows.

a. Optimal real analog wavelet construction

a.i Marr-like analog wavelet base

To demonstrate the construction of optimal analog wavelet bases, we first discuss how to design Marr-like analog wavelet base. Marr wavelet is a favorite choice in many signal processing applications. The Marr wavelet $\psi(t)$ is the second derivative of a Gaussian probability density function:

$$\psi(t) = (1-t^2)e^{-\frac{t^2}{2}}, -\infty < t < \infty \qquad (19)$$

Select the time-shift $t_0 = 4$, get time-reversed and time-shifted Marr wavelet $\psi(4-t)$. Let $\psi_{A1}(t)$ be the Marr-like analog wavelet to be designed and the order of analog wavelet filter N be 9, then the parameterized class of functions $\psi_{A1}(-t)$ given by

$$\psi_{A1}(-t) = x_1 e^{x_2 t} + x_3 e^{x_4 t}\sin(x_5 t) + x_6 e^{x_4 t}\cos(x_5 t) + a_7 e^{x_8 t}\sin(x_9 t) + x_{10} e^{x_8 t}\cos(x_9 t) + x_{11} e^{x_{12} t}\sin(x_{13} t) + x_{14} e^{x_{12} t}\cos(x_{13} t) + x_{15} e^{x_{16} t}\sin(x_{17} t) + x_{18} e^{x_{16} t}\cos(x_{17} t) \quad (t \geq 0) \qquad (20)$$

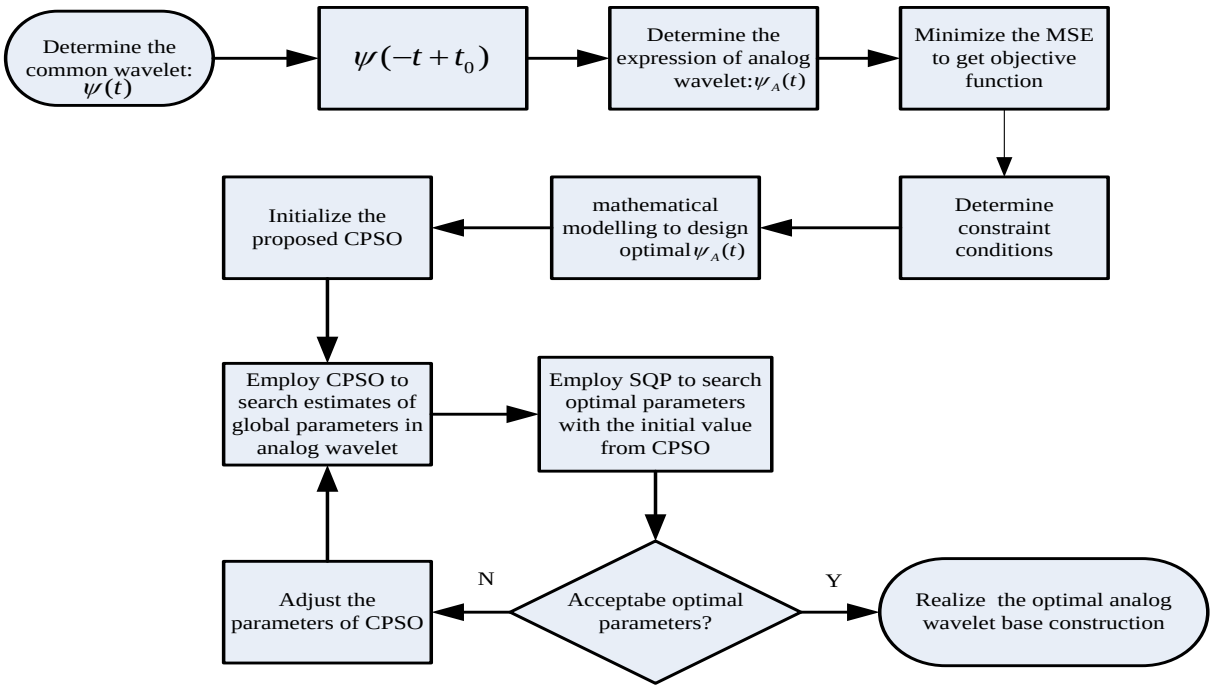

Figure 3. Construction strategy of optimal analog wavelet bases

Note that choice of order of wavelet filter involves an important trade-off between optimal solution and complexity of filter circuits. If N is chosen too small, the designed analog wavelet may be far away from the versatile wavelet. On the other hand, if N is chosen too large, a more complex analog IC is demanded to realize wavelet transform. We define the distance between $\psi_{A1}(-t)$ and $\psi(t-4)$:

$$D(\boldsymbol{x}) = \left\|\psi_{A1}(-t) - \psi(t-4)\right\|^2 = \int_0^{\infty} [\psi_{A1}(-t) - \psi(t-4)]^2 \, dt \qquad (21)$$

where $\boldsymbol{x} = (x_1 \quad x_2 \quad x_3 \cdots x_{18})^T$ is an undetermined parameter vector. To sample $D(\boldsymbol{x})$, the fitness function is given:

$$\min F(\boldsymbol{x}) = \min \sum_{n=0}^{1799} [\psi_{A1}(-n\Delta T) - \psi(-(n\Delta T - 4))]^2 \qquad (22)$$

According to analog wavelet stability and admissibility criterion, the optimization model of constructing Marr-like analog wavelet base is described as

$$\begin{cases} \min \quad F(\boldsymbol{x}) \\ s.t. \quad x_2 < 0, x_4 < 0, x_8 < 0, x_{12} < 0, x_{16} < 0 \\ \dfrac{x_1}{x_2} + \dfrac{-x_3 x_5 + x_4 x_6}{{x_4}^2 + {x_5}^2} + \dfrac{-x_7 x_9 + x_8 x_{10}}{{x_8}^2 + {x_9}^2} \\ + \dfrac{-x_{11} x_{13} + x_{12} x_{14}}{{x_{12}}^2 + {x_{13}}^2} + \dfrac{-x_{15} x_{17} + x_{16} x_{18}}{{x_{16}}^2 + {x_{17}}^2} = 0 \\ \boldsymbol{x} = (x_1 \quad x_2 \quad x_3 \cdots x_{18})^T, \; x_i \in \boldsymbol{R} \end{cases} \tag{23}$$

This is a nonlinear constrained optimization question. Using the proposed hybrid algorithm to solve equation (23), the parameters for CPSO are set as: Population size I =100, Inertia weight factor $w_{\min} = 0.4, w_{\max} = 0.9$, acceleration constant $c_1 = c_2 = 2$, maximum iteration N =9000, chaotic iteration number G=100, premature parameter $\eta = 0.025$. The position and the velocity of the i th particle and the fitness function of corresponding sampling point in the nth iteration are denoted by $\boldsymbol{x}_i^{(n)} = (x_1, x_2 \cdots x_{18})_i^{(n)}$, $\boldsymbol{V}_i^{(n)}$ and $F(\boldsymbol{x}_i^{(n)}) = E(\boldsymbol{x}^{(n)})$ respectively. Its local best position and the global best position of the particle swarm are denoted as $\boldsymbol{P}_i$ and $\boldsymbol{P}_g$ respectively. The maximum iteration for local SQP is set as M =1000. Then, The CPSO optimization program is run first in MATLAB 7.1. Because CPSO is a stochastic algorithm, it is difficult to guarantee a global optimal solution only by a certain experiment. Here, the number of experiments is set to 20. After finishing many times test, the best estimates of the global solution $\boldsymbol{x}^0 = (x^0{}_1 \quad x^0{}_2 \quad x^0{}_3 \cdots x^0{}_{18})^T$ are selected, which is shown in Table 2. The search process of CPSO for the results is given in Figure 4. Then, local SQP optimizer is run with the initial values $\boldsymbol{x}^0$, and the optimal parameters $\boldsymbol{x}^* = (x^*{}_1 \quad x^*{}_2 \quad x^*{}_3 \cdots x^*{}_{18})^T$ of Marr-like analog wavelet base are finally achieved. Experimental results are shown in Table 3. To replace the parameters in equation (20) with $\boldsymbol{x}^*$ in Table 3, the following Marr-like analog wavelet base and filter transfer function (Laplace transform of $\psi_{A1}(-t)$) can be obtained.

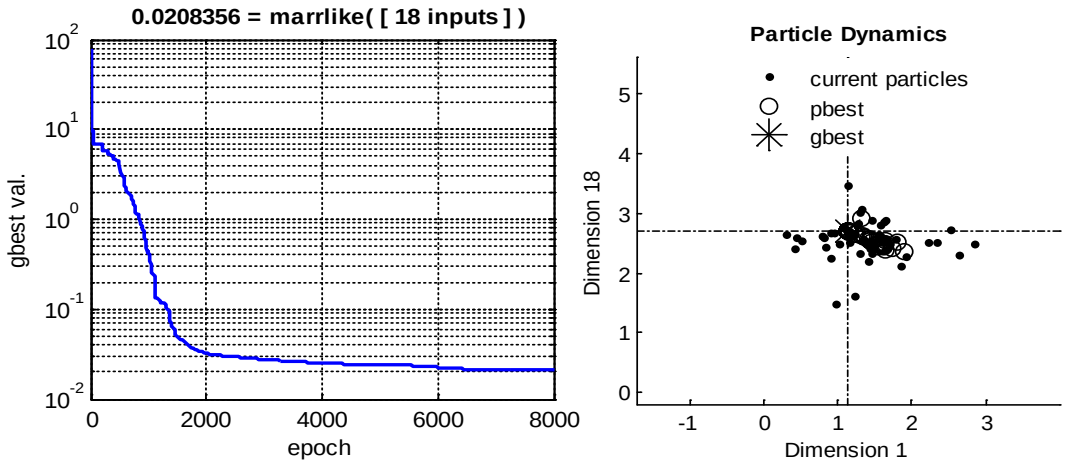

Figure 4. Search process of CPSO for Marr-like analog wavelet

Marr-like analog wavelet base-$\psi_{A1}(t)$:

$$\begin{aligned}\psi_{A1}(t) = &-1.277e^{0.5559t} - 0.7839e^{0.6923t}\sin(1.5376t) + 10.16e^{0.6923t}\cos(1.5376t) - 5.523e^{0.6533t}\sin(0.8171t) \\ &- 5.4571e^{0.6533t}\cos(0.8171t) + 3.1099e^{0.6675t}\sin(2.2809t) - 3.4948e^{0.6675t}\cos(2.2809t) \\ &- 0.6426e^{0.5593t}\sin(3.1158t) + 0.0609e^{0.5593t}\cos(3.1158t) \qquad (t \le 0) \\ \text{Admissibility condition}: &\int_{-\infty}^{\infty}\psi_{A1}(t)dt = 2.415\times10^{-15}\end{aligned} \tag{24}$$

Marr-like analog wavelet filter-$H_{A1}(s)$ **(**N=9**)**:

$$H_{A1}(s) = \frac{-0.0087s^8 + 0.1178s^7 - 1.8405s^6 + 8.4464s^5 - 47.829s^4 + 100.258s^3 - 259.412s^2 + 3.382s}{s^9 + 5.7s^8 + 32.37s^7 + 101.6s^6 + 271.56s^5 + 487.54s^4 + 683.46s^3 + 625.13s^2 + 374.8s + 97.91} \tag{25}$$

Where $H_{A1}(s)$ is the wavelet filter to realize $\mathrm{WT}_{xA}(1,\tau)$ under scale 1. By the theory of Laplace transform, the transfer function of analog wavelet filter under certain scale a is expressed as $\sqrt{a}H_{A1}(as)$. The ime-domain waveform of Marr-like analog wavelet in Figure 5 and the magnitude of frequency response in Figure 6 show the constructed analog wavelet base possess finite support both in time domain and frequency domain. Because Marr-like analog wavelet approaches Mar wavelet very well with MSE=0.0021, it inherits the excellent qualities of Mar wavelet. Meanwhile $\int_{-\infty}^{\infty}\psi_{A1}(t)dt = 2.415\times10^{-15} \approx 0$ and $a_2, a_4, a_8, a_{12}, a_{16} < 0$ demonstrate $\psi_{A1}(t)$ satisfies the admissibility condition and stable condition.

Table 2: Estimates of the global solution x^0 from CPSO ($\psi_{A1}(t)$)

i	x^0_i	i	x^0_i	i	x^0_i
1	-0.0561	7	-1.1791	13	-2.4678
2	-0.1998	8	-0.3967	14	-0.4662
3	0.093	9	-0.7917	15	-0.6442
4	-0.4752	10	-1.2784	16	-1.402
5	-1.5458	11	1.9627	17	-2.7045
6	3.8367	12	-0.4813	18	-2.0219

MSE between $\psi_{A1}(t)$ and $\psi(4-t)$: 0.0208

Table 3: Optimum x^*_i from SQP ($\psi_{A1}(t)$)

i	x^*_i	i	x^*_i	i	x^*_i
1	-1.2772	7	-5.523	13	-2.2809
2	-0.5559	8	-0.6533	14	-3.4948
3	-0.7839	9	-0.8171	15	-0.6426
4	-0.6923	10	-5.4571	16	-0.5593
5	-1.5376	11	3.1099	17	-3.1158
6	10.1595	12	-0.6675	18	0.0609

MSE between $\psi_{A1}(t)$ and $\psi(4-t)$: 0.00091348

Using the similar method, some other real optimal analog wavelet bases have been designed as follows:

a.ii Gaussian-like analog wavelet base

Gaussian wavelet: $\psi(t) = -1.7864te^{-t^2} \quad (-\infty < t < \infty)$

Gaussian -like analog wavelet base-$\psi_{A2}(t)$:

$$\begin{aligned}\psi_{A2}(t) &= 2.5e^{0.95t} - 1.746e^{0.76t}\sin(2.76t) - 0.32e^{0.76t}\cos(2.76t) + \\ &\quad 4.735e^{0.896t}\sin(1.33t) - 2.17e^{0.896t}\cos(1.33t) \qquad (t \le 0) \\ \text{Admissibility condition}: &\int_{-\infty}^{\infty}\psi_{A2}(t)dt = 5.55\times10^{-17}\end{aligned} \tag{26}$$

Gaussian -like analog wavelet filter- $H_{A2}(s)$ (N=5):

$$H_{A2}(s)=\frac{0.014s^4-1.597s^3+3.727s^2-30.89s}{s^5+4.257s^4+16.618s^3+31.35s^2+38.65s+19.92} \tag{27}$$

a.iii Morlet-like analog wavelet base

Morlet wavelet: $\psi(t)=\cos(5t)e^{-0.5t^2} \quad -\infty<t<\infty$

Morlet -like analog wavelet base- $\psi_{A3}(t)$:

$$\begin{aligned}\psi_{A3}(t)=&[(4.81e^{0.77t}+1.713e^{0.739t}\sin(0.89t)-5.68e^{0.739t}\cos(0.89t)-\\&0.749e^{0.619t}\sin(1.88t)+0.88e^{0.619t}\cos(1.88t))]\cdot\cos(5t+15)\quad(t\le 0)\\ \text{Admissibility condition}:&\int_{-\infty}^{\infty}\psi_{A3}(t)dt=2.51\times10^{-17}\end{aligned} \tag{28}$$

Morlet -like analog wavelet filter- $H_{A3}(s)$ (N=10):

$$H_{A3}(s)=\frac{-0.01s^9+0.11s^8-2.88s^7+18.77s^6-74s^5+254.4s^4+4883s^3-10482s^2+34459s}{s^{10}+6.97s^9+155.55s^8+787.28s^7+8582s^6+30633s^5+208060s^4+481500s^3+2175400s^2+2543600s+7582200} \tag{29}$$

The time-domain waveforms and frequency responses of constructed these optimal analog wavelets are given in Figure 7-10 respectively.

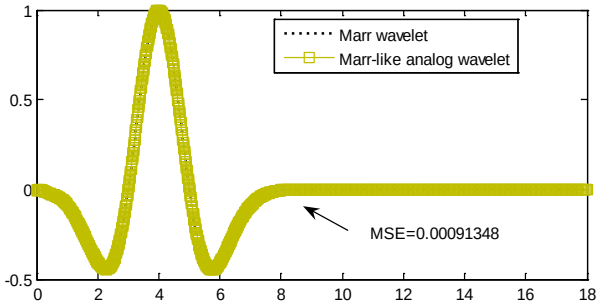

Figure 5. Time-domain waveform of $\psi_{A1}(-t)$

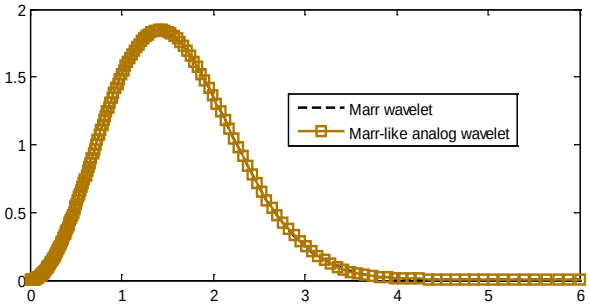

Figure 6. Frequence response of $H_{A1}(s)$

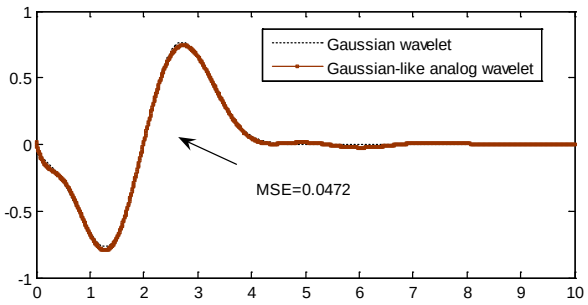

Figure 7. Time-domain waveform of $\psi_{A2}(-t)$

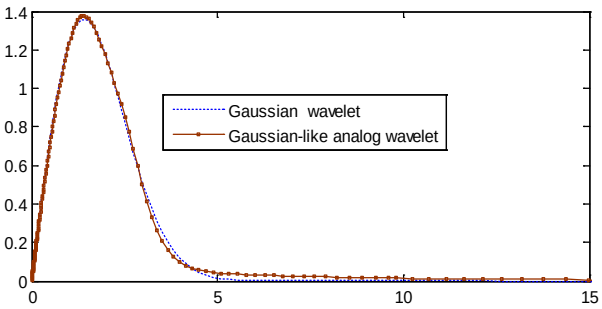

Figure 8. Frequence response of $H_{A2}(s)$

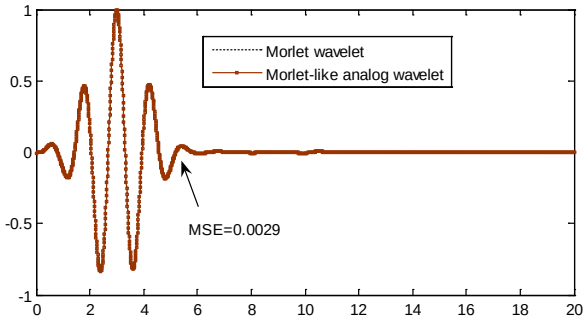

Figure 9. Time-domain waveform of $\psi_{A3}(-t)$

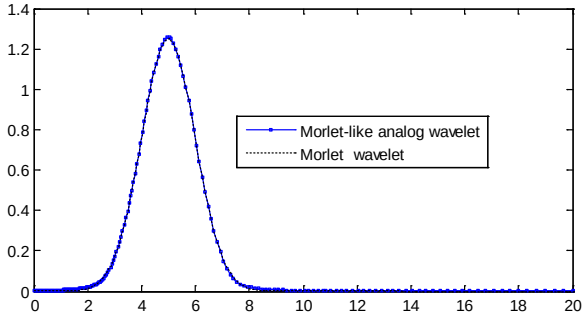

Figure 10. Frequence response of $H_{A3}(s)$

b. Performance evaluation

To illustrate the performance of the proposed method for constructing optimal analog wavelet bases, we investigated the relation of analog wavelet filter orders to the approximate error and the wavelet admissibility condition. Some experiments were conducted upon constructing three sorts of optimal analog wavelet bases with various orders. The experimental result data of Gauss-like analog wavelet, Morlet-like analog wavelet, and Marr-like analog wavelet are given in Tab.4-6 respectively. The relation curves between orders and the approximate error in Fig. 11- 13 show approximate errors always decrease as filter orders become larger. This is because higher order results in more accurate and sophisticated optimization model in equation (12). Given an accurate model, the proposed hybrid algorithm always seeks out the global high-precision solution. However, it is not always feasible to get more optimal analog wavelet by continually increasing the order. The relation of orders to the wavelet admissibility condition shown in Fig.14-16 confirms this. The monotonically increasing curve in Fig.16 illustrates that increasing order will degrade the admissibility condition of Morlet-like analog wavelet. Such as Morlet-like analog

wavelet with order 12, MSE is on the level of 10^{-4} but the admissibility condition on the level of 10^{-7} is still far away the desired value 0 in low order wavelet with larger MSE.For the sake of complex constrained optimization problem, we can't meet MSE and admissibility condition simultaneously. There is always a trade-off between MSE and admissibility condition and our experimental result data provide a reference for the optimal analog wavelet design.

We also compare our method with the state-of-the-art in designing analog wavelet, namely L2 approximation method [26], network function method [23], [25], differential evolution method [30] and simulated annealing method [31].The relation curve also is given in Fig.11-13. For low order analog wavelet, L2 approximation method is in the ascendant, especially for Marr-like and Morlet-like wavelets. But For high order analog wavelet, our method is superior to the other methods. Applying the CPSO algorithm, we have successfully overcome the problem in [26], [25] and [31] that an improper initial value will result the local optimum. The use of SQP algorithm guarantees the accuracy of optimal solution.

Table 4. Results of optimal Gauss-like analog wavelet with various orders

Order	Optimal parameters $\boldsymbol{x}^* = (x^*_1, x^*_2, \cdots)$ in analog wavelet	MSE	Admissibility condition
5	(2.5046,-0.946,1.7458,-0.7593,2.7601,-0.3195,-4.7347,-0.896, 1.3294, -2.171)	0.0472	5.55e-17
6	(4.2135,-0.9427,0.7136,-3.9403,0.3453,-0.8681,-3.4150,-0.9801,0.7027, -0.9818,2.0061,4.8399)	0.0041	2.48e-8
7	(0.7431,-0.7800,-0.5701,-0.9368,3.4553,-0.9153,-0.9797,-0.8952,-0.9251, -4.3375,-0.6989,-0.9965,-2.1360,4.4316)	0.0036	6.2e-7
8	(4.2773,-1.1959,2.9009,-3.5686,1.7549,-0.8087,0.3695,1.8968,0.2370,-1.7156,-3.6027,2.5709,7.9810,-1.0967,-1.4645,-0.9734)	0.0028	1.07e-7
10	(3.6510,-2.6285,-0.3092,2.0647,2.7263,-0.8760,0.7304,-3.8122,1.1089, -0.6774,-1.6236,0.2033,-2.6920,-0.9739,-2.5390,1.4423 -0.6565,-0.9954, 3.8415,0.0358)	0.0017	6.8e-7

12	(-3.0498,-0.8455,-0.5633,-0.9414,-1.5220,-0.7367,1.4656,0.4735,-1.5039, -0.8142,1.9832,1.4677,-2.9995,-2.2083,3.1065,-1.7487,-4.1002,-1.2691,-2.9493,-1.8700,-0.3216,-1.5653,3.8567,2.5573)	0.00083	2.103e-9

Table 5. Results of optimal Marr-like analog wavelet with various orders

Order	Optimal parameters $\boldsymbol{x}^* = (x^*_1, x^*_2, \cdots)$ in analog wavelet	MSE	Admissibility condition
5	(1.5093,-1.149,-2.0658,-0.3386,1.191,-0.3842,0.9354,-0.3125, 2.0426, -0.9757)	1.05	0
6	(-0.4346,-0.3475,0.9838,-1.6504,1.8897,-0.4183,1.7258,1.6483,0.8491,-0.3646 -2.5271,-0.0729)	0.21	0
7	(-0.1144,-0.2557,1.0929,-0.40,-2.4774,-0.26,-1.9753,-0.4762,-1.6569,2.9117, -0.548,-0.4443,-0.8937,-2.6129)	0.0806	0
8	(-29.8211,-0.845,1.4219,5.6572,-1.2556,-0.5304,2.6319,1.2323,24.8199,-0.844,1.7063,-9.4782,-2.46,-0.5291,-0.5625,2.6146)	0.0207	7.5e-9
10	(8.6315,-2.0442,2.4847,0.0942,-2.3096,-0.7499,0.4105,11.824 ,-1.4686,-0.6908,-3.0935, -0.1844,20.769,-0.7855,-1.2481,1.8219,-0.0762,-0.8003,-2.1072,-13.5564)	0.00056	2.66e-8
12	(-3.0397,-1.4765,-2.4955,-18.2849,2.6465,-0.8695,1.5359,31.4718,13.1634,-0.7754,0.5745,15.9316,-17.4771,-0.9416,2.4522,7.8356,-11.5649,-1.4333,0.669,-36.3192,0.3121,-0.7428,-3.4430 ,-0.6401)	0.00034	1.59e-10

Table 6. Results of optimal Morlet-like analog wavelet with various orders

Order	Optimal parameters $\boldsymbol{x}^* = (x^*_1, x^*_2, \cdots)$ in analog wavelet	MSE	Admissibility condition
5	(1.9548,-0.3308,0.5301,-0.6596,-0.5394,-15.8213)	1.1	0
6	(1.8494,-0.4666,-0.9625,-0.391,1.0468,-1.4535)	0.41	0
7	(1.9145,-0.4832,0.936,-0.4112,1.0240,-1.6404,0, -0.0008)	0.0842	3.46e-18

8	(1.1707,-0.4878,-1.477,0.8262,-4.7917,-0.5964,-0.4718,-0.8629,0.0469)	0.0257	1.27e-17
10	(4.8141,-0.7705,1.7134,-0.739,-0.8994,-5.6811,0.7495,-0.619,1.8803,0.8807)	0.0029	2.51e-17
12	(-5.8282,-2.304,9.4056,-0.9102, -1.0298,-6.1537,-1.2851,-0.7518,-2.1017,-0.2955,12.2828,-0.9721)	0.00053	1.44e-9

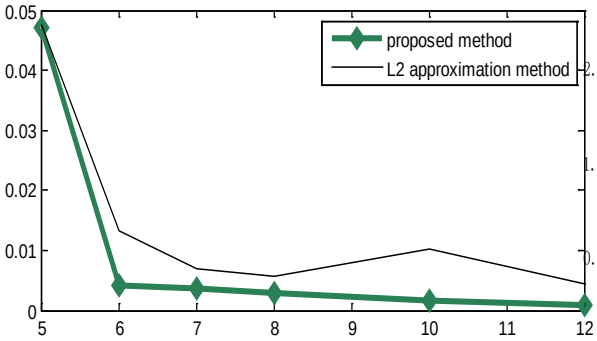

Figure 11. Order and MSE of Gauss-like analog wavelet

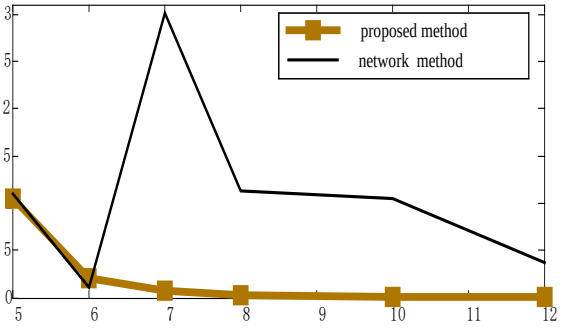

Figure 12. Order and MSE of Marr-like

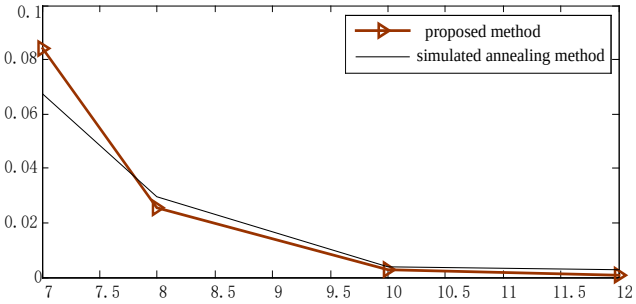

Figure 13. Order and MSE of Morlet-li analog wavelet

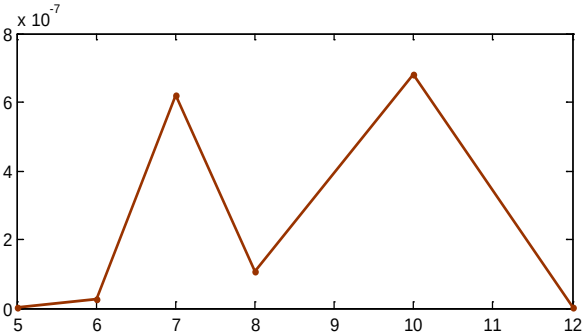

Figure 14. Order and Admissibility condition of Gauss –like analog wavelet

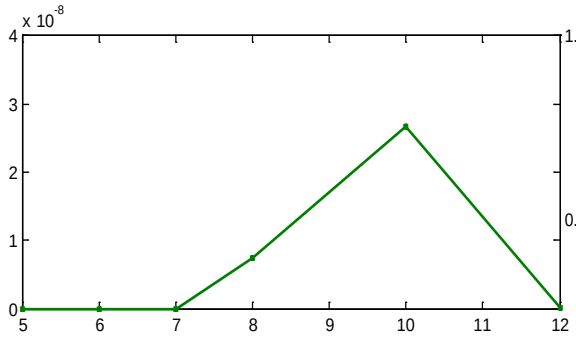

Figure15. Order and Admissibility condition of Marr-like analog wavelet

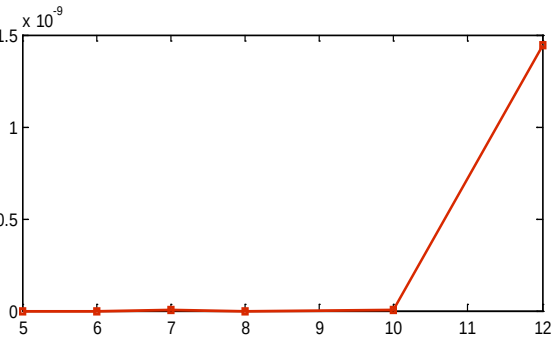

Figure 16. Order and Admissibility condition of Morlet-like analog wavelet

VI. CONCLUSION

Based on the proposed hybrid optimization algorithm and the general framework for designing analog wavelets, a series of optimal analog wavelet bases including Marr-like analog wavelet base, Gaussian-like analog wavelet base, Morlet-like analog wavelet base, have been constructed. These constructed analog wavelets possess optimal local time-frequency characteristics and most of properties in them are almost close to the properties owned by corresponding versatile wavelets. Currently, we are working on utilizing methods in this paper to construct orthogonal analog wavelet bases. The further work is to design analog wavelet transform chip utilizing advanced analog circuit technology for some practical application such as sensor networks and next-generation cochlear implants.

ACKNOWLEDGMENTS

The Authors thank the Natural Science Foundation of Hunan Province of China (grant no. 11JJ3078), China Postdoctoral Science Foundation (grant no. 2012M521215), The Research Foundation of Education Bureau of Hunan Province,China(Grant No. 14A062)， and National Natural Science Funds of China for Distinguished Young Scholar under (grant no. 50925727)

REFERENCES

[1] S. Mallat, A Wavelet Tour of Signal Processing. New York: Academic, 1999.

[2] Walnut, David F, An Introduction to Wavelet Analysis. Boston: Birkhäuser Press, 2004.

[3] Su Hua, Zhang Tianyuan, Zhang Ning, “Acoustic emission based defects monitoring of Three-Dimensional braided composites using wavelet network”, International Journal on Smart Sensing and Intelligent System, vol. 9, no. 2, 2016, pp.780-798.

[4] Zhang Ning, Zhu Jinfu, “Study on image compression and fusion based on the wavelet transform technology”, International Journal on Smart Sensing and Intelligent System, vol. 8, no. 1, 2015, pp. 480-496.

[5] H. Hashim, S. Ramli, N. Wahi, M. S. Sulaiman, N. Hassan, “Recognition of Psioriasis Features via Daubechies D8 Wavelet Technique ”, International Journal on Smart Sensing and Intelligent System, vol. 6, no. 2, 2013, pp. 711-732.

[6] I. F. Akyildiz, T. Melodia, and K. R. Chowdhury, “A survey on wireless multimedia sensor networks,” Computer Networks, vol. 51, no. 4, 2007, pp. 921-960.

[7] Rein. S, Reisslein. M, “Low-memory wavelet transforms for wireless sensor networks: A tutorial,” IEEE Communications Surveys & Tutorials, vol. 13, no. 2, 2011, pp. 291-307.

[8] R. Sarpeshkar, C. Salthouse, J. J. Sit, etc., “An ultra-low-power programmable analog bionic ear processor,” IEEE Trans. Biomed. Eng., vol. 52, no. 4, 2005, pp. 711-727.

[9] V. Gopalakrishna, N. Kehtarnavaz, P. C. Loizou, “A recursive wavelet-based strategy for real-time cochlear implant speech processing on PDA platforms,” IEEE Trans. Biomed. Eng., vol. 57, no. 8, 2010, pp. 2053-2063.

[10] S. A. P. Haddad, R. Houben, and W. A. Serdijn, “Analog wavelet transform employing dynamic tranlinear circuits for cardiac signal characterization,” in Proc. IEEE Int. Symp. Circuits Syst. (ISCAS), 2003, vol. 1, pp. 121-124.

[11] M. W. Phyu , Y. Zheng , B. Zhao , L. Xin and Y. S. Wang, “A real-time ECG QRS detection ASIC based on wavelet multiscale analysis,” Proc. IEEE Asian Solid-State Circuit Conf., pp. 293-296, 2009.

[12] Hoon-Ki Kim,Yu-Ri Kang,Gil-Su Kim ,etc., “Design of Wavelet-Based ECG Detector for Implantable Cardiac Pacemakers,” IEEE Trans. Biomedical Circuits and Systems, vol. 7, no. 4, 2013, pp. 426-436.

[13] F.Baskaya, S. Reddy, S.K. Lim, “Placement for Large-scale Floating-Gate Field Programmable Analog Arrays,” IEEE Trans. VLSI, Vol. 14, No. 8, 2006, pp.906-910.

[14] T.S. Hll, C.M. Twigg, J.D. Gray, P. Hasler, “Large-scale field-programmable analog arrays for analog signal processing,” IEEE Trans. Circuits Syst. I, vol. 52, no. 11, 2005, pp. 2298-2307.

[15] A. Basu , S. Brink , C. Schlottmann , S. Ramakrishnan , C. Petre , S. Koziol , F. Baskaya , C.

M. Twigg and P. Hasler, “A floating-gate-based field-programmable analog array,” IEEE J. Solid-State Circuits, vol. 45, , 2010, pp. 1781-1794.

[16] D. FernÃ¡ndez , L. MartÃnez-Alvarado and J. Madrenas, “A translinear, log-domain FPAA on standard CMOS technology,” IEEE J. Solid-State Circuits, vol. 47, 2012, pp. 490-503.

[17] W. Fu , J. Jiang , X. Qin , T. Yi and Z. Hong, “A reconfigurable analog processor using coarse-grained heterogeneous configurable analog blocks for field programmable mixed-signal processing,” Analog Integr. Circuits Signal Process., vol. 68, no. 1, 2011, pp. 93-100.

[18] Moreira-Tamayo O, Pineda de Gyvez J, “Analog computation of wavelet transform coefficients in real-time,” IEEE Trans. Circuits Syst. I, vol. 44, no. 1, 1997, pp. 60-70.

[19] T. R. Edwards and M. D. Godfrey, “An analog wavelet transform chip,” ICNN Proc., pp.1247 -1251, 1993.

[20] He Yigang, Huang Qingxiu, “Continuous Wavelet transform synthesis using instantaneous companding circuits,” Proc of world multiconference on systemics, Cybernetic and Informatics, proceedings, Orlando, USA., pp. 316-321, 2003.

[21] Lin, W. Ki, T. Edwards, and S. Shamma, “Analog VLSI implementations of auditory wavelet transforms using switch-capacitor circuits,” IEEE Trans. Circuits Syst. I, vol. 41, no. 9, 1994, pp. 572-583.

[22] M. Liu, Q. Hu, and Y. He, “A novel analog VLSI implementation of wavelet transform based on SI circuits,” in Proc. Congr. Image Signal Process. (CISP), May 2008, vol. 1, pp. 317–323.

[23] W. Zhao, Y.-G. He, J. Huang, Y. Y. Xie, and Y. Zhang, “Analogue VLSI implementations of wavelet transform based on switched-current technology,” in Proc. Int. Conf. Wavelet Anal. Pattern Recognit. (ICWAPR), Nov. 2007, vol. 4, pp. 1787–1792.

[24] M.A. Gurrola-Navarro, G. Espinosa-Flores-Verdad, “Analogue wavelet transform with single biquad stage per scale,” Electronics Letters, vol. 46, no. 9, 2010,pp. 616-618.

[25] Wenshan Zhao,Yigang He, Realization of wavelet transform using switched-current filters, Circuits Systems and Signal Processing, vol. 71, no. 10, 2012, pp. 571-581.

[26] J. M. H. Karel, R. L. M. Peeters, R. L. Westra, S. A. P. Haddad, and W. A. Serdijn, “An L2 -based approach for wavelet approximation,” in Proc. CDC-ECC, 2005.

[27] L Hongmin, H Yigang, Y Sun, “Detection of cardiac signal characteristic point using log-domain wavelet transform circuits,” Circuits Systems and Signal Processing, vol. 27, no. 10,

2008, pp. 683-698.

[28] Hongmin Li, Heyi Gang,Guoyun Zhang , “Log-domain implementation of analog wavelet filters”, Intelligent Control and Information Processing (ICICIP), 2010 International Conference on, pp. 187-190, Aug. 2010.

[29] M.A. Gurrola-Navarro, G. Espinosa-Flores-Verdad, “Analogue wavelet transform with single biquad stage per scale,” Electronics Letters, vol. 46, no. 9, 2010, pp. 616-618.

[30] M. Li, Y. He and Y. Long, “Analog VLSI implementation of wavelet transform using switched-current circuits,” Analog Integrated Circuits and Signal Processing, vol. 71, no. 5, 2012,pp. 283-291.

[31] Li, M., He, Y., “Analog wavelet transform using multiple-loop feedback switched-current filters and simulated annealing algorithms,” International journal of Electronics and Communications, vol. 68, no. 5, 2014,pp. 388-394.

[32] Joseph-Frédéric Bonnans, Numerical Optimization: Theoretical and Practical Aspects, springer press, 2006.

[33] Kennedy J, Eberhart RC, “Particle swarm optimization,” In: Perth, Piscataway. IEEE International Conference on Neural Networks, Australia: IEEE Service Center, pp.1942-1948, 1995.

[34] D. Henderson, S. H. Jacobson, and A. W. Jacobson, “The theory and practice of simulated annealing,” in Handbook of Metaheuristics, Kluwer Academic Publishers Group, pp. 287-319, 2003.

[35] T. Back, Evolutionary Algorithm in Theory and Practice, Oxford Univ. Press, 1996.

[36] Madhuri, K. Deep, “A state-of-the-art review of population-based parallel meta-heuristics,” World Congress on Nature & Biologically Inspired Computing, pp. 1604 -1607, Dec. 2009.

[37] F. Van den Bergh, A. P. Engelbrecht, “A Cooperative approach to particle swarm optimization,” IEEE Trans. Evolutionary Computation, vol. 8, no. 3, 2004, pp. 225-239.

[38] B. Liu, L. Wang, Y.H. Jin, F. Tang, D.X. Huang, “Improved particle swarm optimization combined with chaos,” Chaos, Solitons Fractals, vol. 25, no. 5, 2005,pp. 1261-1271.

[39] Mieczyslaw Jessa, “Designing Security for Number Sequences Generated by Means of the Saw tooth Chaotic Map,” IEEE Trans. Circuits Syst. I, vol. 53, no. 5, 2006,pp. 1140-1150.s